Research article

FV-429 induces apoptosis by regulating nuclear translocation of PKM2 in pancreatic cancer cells

Xifan Jin [a],[1], Qi Min [b],[c],[1], Dechao Wang [a], Yi Wang [a], Guangming Li [a], Zhiying Wang [a], Yongjian Guo [a],[**], Yuxin Zhou [a],[*]

[a] State Key Laboratory of Natural Medicines, Jiangsu Key Laboratory of Carcinogenesis and Intervention, China Pharmaceutical University, 24 Tongjiaxiang, Nanjing, 210009, China
[b] Nanjing University of Chinese Medicine, China
[c] Department of Oncology, Huai'an Second People's Hospital, The Affiliated Huai'an Hospital of Xuzhou Medical University, China

A B S T R A C T

Of all malignancies, pancreatic ductal adenocarcinoma (PDAC), constituting 90% of pancreatic cancers, has the worst prognosis. Glycolysis is overactive in PDAC patients and is associated with poor prognosis. Drugs that inhibit glycolysis as well as induce cell death need to be identified. However, glycolysis inhibitors often fail to induce cell death. We here found that FV-429, a derivative of the natural flavonoid wogonin, can induce mitochondrial apoptosis and inhibit glycolysis in PDAC *in vivo* and *in vitro*. *In vitro*, FV-429 inhibited intracellular ATP content, glucose uptake, and lactate generation, consequently leading to mitochondrial dysfunction and apoptosis in PDAC cells. Furthermore, it decreased the expression of PKM2 (a specific form of pyruvate kinase) through the ERK signaling pathway and enhanced PKM2 nuclear translocation. TEPP-46, the activator of PKM2, reversed FV-429-induced glycolysis inhibition and mitochondrial apoptosis in the PDAC cells. In addition, FV-429 exhibited significant tumor suppressor activity and high safety in BxPC-3 cell xenotransplantation models. These results thus demonstrated that FV-429 decreases PKM2 expression through the ERK signaling pathway and enhances PKM2 nuclear translocation, thereby resulting in glycolysis inhibition and mitochondrial apoptosis in PDAC *in vitro* and *in vivo*, which makes FV-429 a promising candidate for pancreatic cancer treatment.

1. Introduction

Pancreatic cancer is a prevalent malignant tumor in the digestive tract. Recently, the incidence rates of pancreatic cancer have significantly increased in China [1,2]. Pancreatic ductal adenocarcinoma (PDAC) cells exhibit an elevated glycolytic flux, glucose uptake rate, and lactate production rate. These metabolic alterations in PDAC tumors support tumor growth, prevent cell apoptosis, and facilitate the development of drug resistance [3].

Apoptosis, a highly regulated form of cell death, is essential for the appropriate development and maintenance of normal tissues

* Corresponding author.
** Corresponding author.
   E-mail addresses: guoyj@cpu.edu.cn (Y. Guo), zyxspain@hotmail.com (Y. Zhou).
[1] These authors contributed equally.

[4]. The intrinsic pathway of apoptosis is known as the mitochondrial apoptosis pathway [5]. This pathway involves permeabilization of the mitochondrial outer membrane (MOMP), which triggers the release of cytochrome *c* (Cyt *c*) into the cytoplasm. The release of MOMP and Cyt *c* induces apoptotic body formation and Caspase-3 activation [6]. Tumor cells can escape apoptosis through various mechanisms.

Many cancer cells exhibit the Warburg effect, which results in increased glycolysis [7]. By relying on glycolysis, cancer cells reduce their dependence on mitochondria and oxidative phosphorylation, which can generate high levels of reactive oxygen species (ROS). ROS has been associated with cancer since long, and different tumor cells produce higher ROS levels than normal cells [8]. PKM2 is a specific pyruvate kinase (PK) form involved in the "Warburg effect," which is commonly observed in tumor cells [9]. Breviscapine, a flavonoid, inhibits PKM2 aggregation and induces cell cycle arrest and apoptosis in HeLa cells [10], which suggests that PKM2 has a role in cell apoptosis. TEPP-46 is a small molecule serving as an agonist for PKM2. It prevents PKM2 nuclear translocation by stabilizing the interaction between PKM2 subunits and increasing its activity [11,12]. ERK, a protein kinase, influences PKM2 expression [13]. Resveratrol, a flavonoid, induces PKM2-mediated targeted apoptosis [14]. It also affects glucose metabolism in various cancer cells by regulating PKM2 expression through the activation of the ERK1/2 signaling pathway. These studies highlight the significance of PKM2 in cancer metabolism and its potential as a therapeutic target for cancer treatment.

Wogonin and its derivative compound, FV-429, possess a range of interesting biological activities. Wogonin, extracted from *Scutellaria baicalensis*, exhibits antioxidant, antiviral, and anti-inflammatory properties [15,16]. On the other hand, FV-429, a modified form of baicalein, can potentially affect the mitochondrial function and tumor cell metabolism by inhibiting aerobic glycolysis [17]. However, until now, the specific effects of FV-429 on PDAC cells have not been studied. To address this gap, we here investigated the key molecular mechanisms of aerobic glycolysis and cell survival in PDAC cells. Our findings revealed that FV-429 effectively induces apoptosis and inhibits glycolysis in the PDAC cells. This research offers valuable insights into the potential therapeutic applications of FV-429 for PDAC treatment.

2. Materials and methods

2.1. Cell lines, culture conditions and reagents

Human pancreatic cancer cells BxPC-3, PANC-1, MiaPaCa-2, Capan-2 and human pancreatic cells HPNE were purchased from the cell bank of Shanghai Institute of Biochemistry and Cell Biology. Cells were configured in RPMI-1640 medium, DMEM medium and McCoy's 5A medium.

FV-429 (Molecular formula: $C_{23}H_{25}NO_7$, molecular weight: 429), orange powder. FV-429 was dissolved with DMSO and stored in $-80\,°C$ refrigerator. MTT (3 - (4, 5 - dimethylthiazol - 2 - yl) - 2, 5 - diphenyltetrazolium bromide) was purchased from Sigma. ATP test kit was purchased from Nanjing Biyuntian Biotechnology Co., LTD. Lactic acid detection kit was purchased from Nanjing Kaiji Biotechnology Development Co., LTD. The glucose test kit was purchased from BOXBIO, a company in Beijing. The ECAR test kit, seahorse Energy Metabolizer test kit, was purchased from Agilent Technologies. The ERK signaling pathway activator Phorbol 12-myristate 13-acetate was purchased from CSNpharm. AnnexinV-FITC/PI Apoptosis detection kit was purchased from Novizan Biotechnology Co., LTD. (item No. A211-02). PKM2 activator TEPP-46 was purchased from MCE (MedChemExpress).

Key antibodies of PKM2, ERK1/2, P-ERK1/2, p53, Bax, Bcl 2, caspase9, Histone H3, VDAC, Tubulin and β-actin were gained from Santa Cruz Biotechnology. Cyt *c*, caspase3, cleaved-caspase3, PARP1, anti-rabbit IgG HRP and anti-mouse IgG HRP, were bought from ABclonal Technology. Antibody conjugates were achieved by chemiluminescence (ECL, Thermo Fisher Scientific).

2.2. MTT assay

To determine cell viability, we used MTT assay. Briefly, Cells (8×10^3) were treated by FV-429 for 24 h at different concentrations. After the 24-h treatment period, we added 20 μL of a 5 mg/mL solution of MTT to cells. The cells were then incubated at 37 °C for an additional 3 h to allow the reduction of MTT by viable cells. The absorbance of the final sample product, indicative of cell viability, was examined at 570 nm using a Universal Microplate Reader EL800 (BioTek Instruments, Winooski, VT, USA). Formula (1-OD (experiment)/OD (control) × 100%) used to calculate cell proliferation inhibition rate.

The IC50 value is a measure of the concentration of a substance that is required to inhibit cell viability by 50%. In this case, the Logit method was used to calculate the IC50 value. Graphpad Prism 8.0 software was utilized for the calculation. To ensure accuracy and reliability, each experiment was conducted three times in parallel.

Comprehensively considering the IC50 values of the two cell lines, the three concentrations 20, 40, and 80 μM were preliminarily determined. For the convenience of research, 24 h was chosen as the exposure time. Together with the morphological detection, DAPI staining and apoptosis test, exposure time and concentrations were finally determined.

2.3. CCK8

BxPC-3 cells and PANC-1 cell lines were seeded into 96-well plates at 8000 cells per well overnight and then incubated with FV-429 for 24 h at different concentrations Then 10 μL CCK8 (Vazyme, Nanjing, China) were added to each well and the plates was placed at 37 °C for 2 h. The absorbance measurements of CCK8 were performed in Varioskan multimode microplate spectrophotometer at a wavelength of 450 nm.

2.4. Lactate generation, glucose uptake level and ATP content

The detection kit of lactate generation from KeyGen (Cat number: KGT023) is a commonly kit for measuring the production of lactic acid. Which involved collecting culture medium samples at specific time points and mixing them with lactate assay buffer in a 96-well plate, with 100 μL per well. Then, 100 μL of reaction buffer was added to each well and the plate is putted at 37 °C for 20 min. The lactate generation was measured by spectrophotometer (Thermo, Waltham, MA) at 570 nm. Manufacturer's instructions were used and all measurements were normalized according to the number of cells in each experiment.

The detection kit of ATP from Beyotime Biotechnology (Cat number: S0026) was employed to measure the ATP content in the study. The assay was performed following the instructions provided by the manufacturer. The cells were lysed with Cell Lysis Reagent on ice, followed by 50 μL of Luciferase Reagent added. Luciferase, an enzyme that catalyzes the light-emitting reaction of luciferin and ATP, was utilized to detect and quantify ATP levels. As ATP reacts with luciferin in the presence of luciferase, light emission occurs and is detected by a luminometer or a plate reader.

Glucose content detection kit (BOXBIO, catalog number: AKSU001C) can oxidize glucose to Glucoronic acid according to Glucose Oxidase (GOD), and release H_2O_2. Peroxidase (POD) catalyzed H_2O_2 oxidation of 4-amino-antipyrine coupled phenol to produce red quinone compound. The product had a characteristic absorption peak at 505 nm, and the glucose content could be quantitatively detected through the change of light absorption value. Briefly, cells were collected, then added 450 μL reaction buffer and putted at 37 °C for 15 min. Spectrophotometer (Thermo, Waltham, MA) was used to measure glucose at 505 nm.

2.5. Seahorse analysis extracellular acidification rate (ECAR)

In the ECAR experiment, we first inoculated 1×10^3 cells into each well of an XF96 cell culture plate containing 10% FBSRIPM1640 (Seahorse Bioscience) and grew them for about 8 h. Different dosages of FV-429 were then added and putted in a 37 °C humidifier with 5% CO_2 for 24 h. Sterile ultra-pure water (ddH$_2$O) was added to a generic plate in incubator with 37 °C/non-CO$_2$ for 12 h in advance, and then the ddH$_2$O was changed to a calibration solution prior to assay. Before assay, about 1 h, 10% FBSRIPM1640 was carefully washed off and replaced with hippocampal base medium (PH = 7.4), then finally placed in a 37 °C/non-CO$_2$ incubator for 60 min 37 °C was the prerequisite of all experiments and all seahorse measurements were normalized according to the number of cells.

2.6. Annexin V-FITC/PI staining

To investigate cell death induced by different concentrations of FV-429, we used Annexin V-fluorescein isothiocyanate (FITC)/ Propidium iodide (PI) staining. Briefly, the PDAC cells were treated with different concentrations (20, 40, and 80 μM) of FV-429 for 24 h. Afterward, the cells were incubated with 0.25% trypsin and 0.02% EDTA for 5 min at 37 °C, followed by centrifugation at 1100 rpm for 6 min. The cells were then double-stained with Annexin V-FITC and PI for 9 min at room temperature. Cytometry Cytometer (BD Accuri C6) and Flow Jo version 10 software were used to quantitatively analyze the fluorescence. Cells that exhibited positive staining for both PI and Annexin V-FITC were considered apoptotic.

2.7. Mitochondrial membrane potential and intracellular ROS levels

The mitochondrial membrane potential was detected by the JC-1 (KeyGEN Biotech, Nanjing, China; catalogue #KGA602) using fluorescence-activated flow Cytometer. Different concentrations of FV-429 were traeted on PDAC cells for 24 h. After treatment, the cells were collected and incubated with JC-1 working solution for 20 min at 37 °C in the dark. After incubation with JC-1, the cells were washed twice with JC-1 buffer to remove any unbound dye. The relative fluorescence intensities of the cells were then analyzed using flow Cytometer (BD Accuri C6). Green fluorescence was detected by FL-1 and red fluorescence was detected by FL-2. Data were analyzed by FlowJo version 10.

In this experiment, the evaluation of reactive oxygen species (ROS) generation was conducted using a dye called DCFH-DA (Beyotime Biotechnology, Shanghai, China; catalogue #S0033S). The PDAC cells were treated with FV-429 for a duration of 24 h, followed by trypsinized and centrifuged at 1100 rpm for 5–6 min. After washed with cold PBS twice, the cells were then re-suspended in 10 μM DCFH-DA diluted with serum-free culture medium. The cells were detected for ROS generation by flow Cytometer.

2.8. Western blot

First of all, we collected cells into the centrifuge tube. The cells were lysed by a RIPA buffer supplemented with protease inhibitors and phosphatase inhibitors. Then we centrifuged protein lysates, and it were quantified by the BCA Protein Assay (Thermo Fisher Scientific). Nextly, protein boiled with loading buffer. And SDS-PAGE was added to separated protein samples on ice, then transferred samples into the nitrocellulose membrane. Finally, the membrane was blocked with 3% BSA in PBST for 1.5 h prior to treatment overnight at 4 °C with key antibody, followed by Respective HRP-conjugated secondary antibodies for 1 h at room temperature.

2.9. Immunofluorescence

The PDAC cells in the logarithmic growth stage were injected into the six-well plate with a slide at a rate of 320,000 per well and cultured in a incubator at 37 °C. After 24 h of administration, the supernatant was discarded and rinsed with PBS. The cells were fixed

with 4% paraformaldehyde for 10 min and washed with PBS. Add 0.3% Triton to permeate for 10 min, and then wash with PBS twice. Add 3% BSA to seal for 2 h, and wash with PBS 3 times for 5 min each time. Each tablet was added with 100 μL of 1:100 concentration of primary antibody and incubated at 4 °C overnight. Wash with 10% PBST. Dilute with 1:100 and add fluorescent secondary antibody, incubate at room temperature and avoid light for 40 min, and wash with 10% PBST. The plates containing DAPI quench inhibitor were sealed and then photographed under a confocal laser microscope.

2.10. Separation of mitochondrial and cytoplasmic components, separation of cytoplasmic and nuclear components, extraction of tumor proteins

To dissect mitochondria and cytosolic fractions of cells, we used Cytosol/mitochondria fractionation kit (KeyGen Biotech, China). Briefly, we used FV-429 to treat the cells for 24 h. Nextly, collected cells, blown evenly in a cold mitochondrial lysis buffer and cleaved for 10 min. Cell suspension of 600 g was taken, centrifuged at 4 °C for 10 min, and the nucleus and unbroken cells were taken. The supernatant was then centrifuged at 4 °C at 12,000 g for 20 min to precipitate the mitochondria. The supernatant was wiped off as part of the cytoplasm, and the remaining mitochondrial particles were re-suspended in the extraction buffer. Both samples were dissolved in lyses buffer and stored at −20 °C.

Nuclear protein was extracted by nuclear plasma separation. The cells were treated with FV-429 for 24 h. The lysate was added and the cells were blown with a tail vein needle to chop up the cells. Cell suspension was subjected to centrifuging at 12,000 g for 20 min at 4 °C. The supernatant obtained by centrifugation was cytoplasmic protein. Pellet was washed three times with the lysate, at 12,000 rpm, centrifuged at 4 °C for 3 min, and the obtained precipitation was nuclear protein. The protein concentration was detected by BCA method, 4× loading buffer was added to the samples, denatured at 90 °C for 8 min, then cooled to room temperature and stored at −20 °C.

Extraction of tumor protein. 50 mg tumor samples were taken, 200 μL RIPA lysate (including protease and phosphatase inhibitors) was added, ground, and then transferred to 1.5 mL tube for splitting on ice for 30 min with vortex oscillation every 10 min. After centrifugation at 4 °C for 20 min at 15,000 rpm, the supernatant was collected, the protein concentration was detected by BCA method, 4× loading buffer was added to the samples, denatured at 90 °C for 8 min, then stored at −20 °C.

2.11. Xenograft mouse model and immunohistochemistry

In this experiment, BxPC-3 cells in the logarithmic growth phase were digested and collected. A cell suspension was prepared using normal saline, and the cells were then inoculated under the arm of mice. After approximately 5 days, the mice were randomly divided into different groups: blank group, positive drug group (treated with gemcitabine at a dose of 10 mg/kg), and FV-429 group (treated with FV-429 at a dose of 15 mg/kg). There were 5 mice in each group. FV-429 was administered intravenously every two days and gemcitabine was injected intraperitoneally once a week. After 30 days of treatment, the mice were euthanized, and the tumor blocks were cleaned, photographed, fixed, and then paraffin-embedded and sliced. All mouse experiments were in compliance with the policies of the SFDA (State Food and Drug Administration) of China on Animal Care. All animals received humane care according to the criteria outlined in the Guide for the Care and Use of Laboratory Animals prepared by the National Academy of Sciences and published by the National Institutes of Health. Female athymic nude mice (4–6 weeks old) weighing 18–22 g were purchased from the Academy of Military Medical Sciences of the Chinese People's Liberation Army (Certificate No. SCXK (ZHE) 2019–0004).

Immunohistochemistry, briefly, started with dewaxing. Immersed the slide in xylene 3 times for 5 min each time. Then the water was hydrated in ethanol solutions of different concentrations for 3 min each time. Then it was immersed in ddH$_2$O for 5 min, and then washed in PBS for 2 min. Then the antigen was renovated, cooled to room temperature, left in distilled water for 3 min, and rinsed with PBS for 3 min. The slices were placed in 0.3% TritonX-100 solution for 20 min. Sealer solution (5% serum and 0.5% BSA, prepared with PBS) was added and sealed for 30 min. Then, the tissue surface was dripped with immunohistochemical reagent 1 to remove endogenous HRP, and the tissue was placed at room temperature for 15 min and rinsed with PBS for 5 min. Added the key antibody to the slide, such as caspase3, cleaved-caspase3, Bax, Bcl-2, PKM2 and p53. Putted in tne four-degree efrigerator for the night. The next day we added reagent 2 and reacted at 37 °C for 1 h, then washed with PBST for 3 min, applied antibody 2, added reagent 3, reacted at 37 °C for 20 min. After PBST cleaning, DAB was used for color development. Dyed with hematoxylin solution and rinsed with cold running water, then it returned to blue. Finally, after dehydration, the tablets were sealed and observed under microscope.

2.12. Statistical analysis

The analysis of the data was performed using Graphpad Prism 8.0 software. The values are presented as the Mean ± SD and the statistically significant difference between groups was analyzed using one-way ANOVA and Dunnett's post hoc test. A p-value of less than 0.05 was considered statistically significant. The level of significance is denoted as $*p < 0.05$ and $**p < 0.01$, indicating the degree of significance in the observed differences between groups.

3. Results

3.1. FV-429 inhibited glycolysis and PDAC cells' viability

In the study, the MTT assay was used to assess the inhibitory effect of FV-429 (Fig. 1A) on the viability of PDAC cell lines.
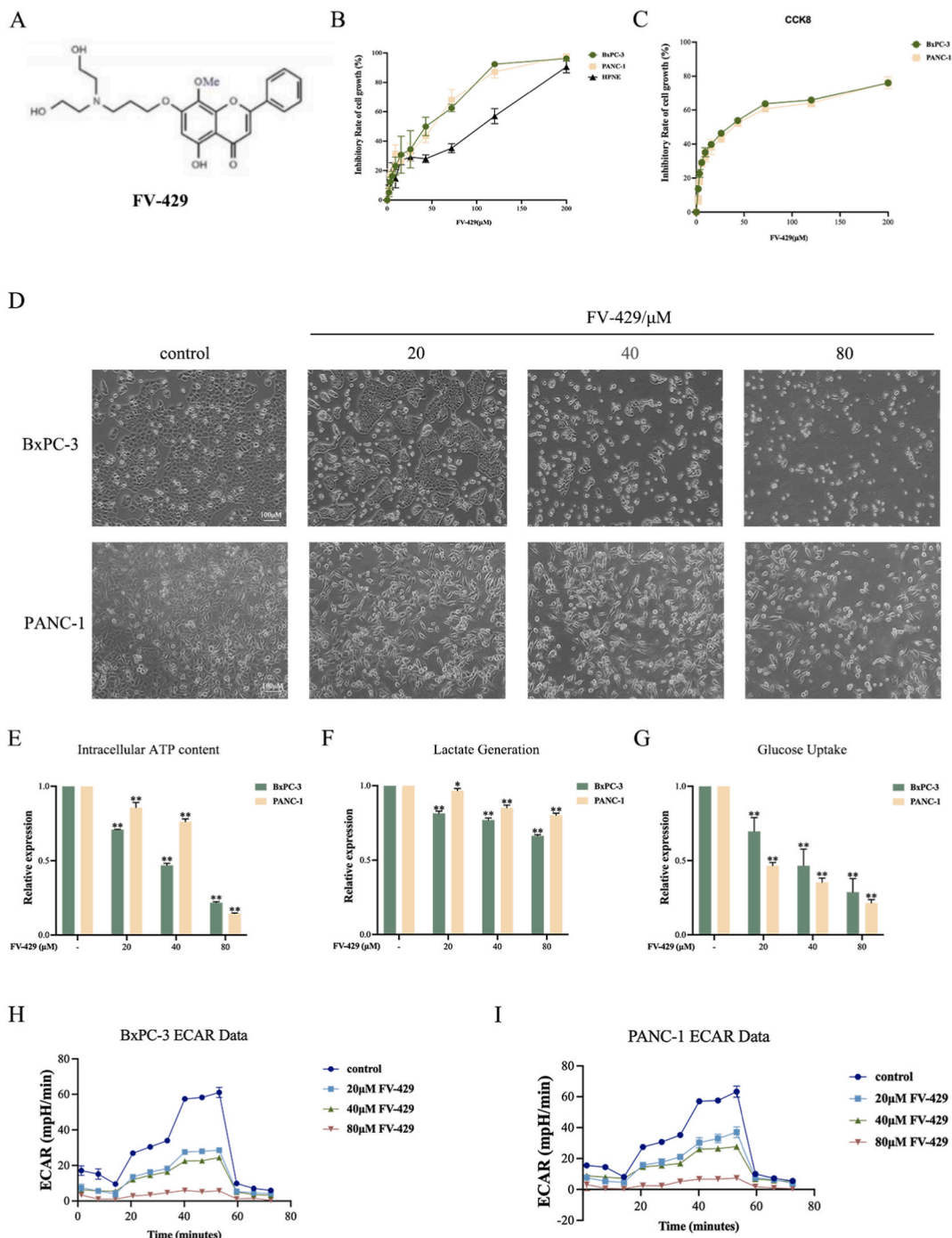
Fig. 1. FV-429 inhibited glycolysis and viability of PDAC cells. (A) FV-429 molecular structure ($C_{23}H_{25}NO_7$, molecular weight = 429) transformed from Wogonin. (B) MTT assay was used to detect the decrease in percentage viability of BxPC-3, PANC-1 and HPNE cells, following treatment with increasing concentrations of FV-429 (0–200 μM) for 24 h. (C) The CCK8 assay of the PDAC cells. (D) Morphology was used to observe the morphology of PDAC cells BxPC-3 and PANC-1 by FV-429 after FV-429 (20, 40, 80 μM) treatment for 24 h. (E) ATP production was assayed by ATP assay kit. (F) Production of lactic acid was assayed by Lactic Acid production Detection kit. (G) Glucose uptake was measured using the Glucose Assay Kit. (H, I) ECAR was measured by XF96 Extracellular Flux Analyzer. Data were presented as mean ± SD of three independent experiments performed in triplicates. Significant difference: *p < 0.05, **p < 0.01, compared with the control.
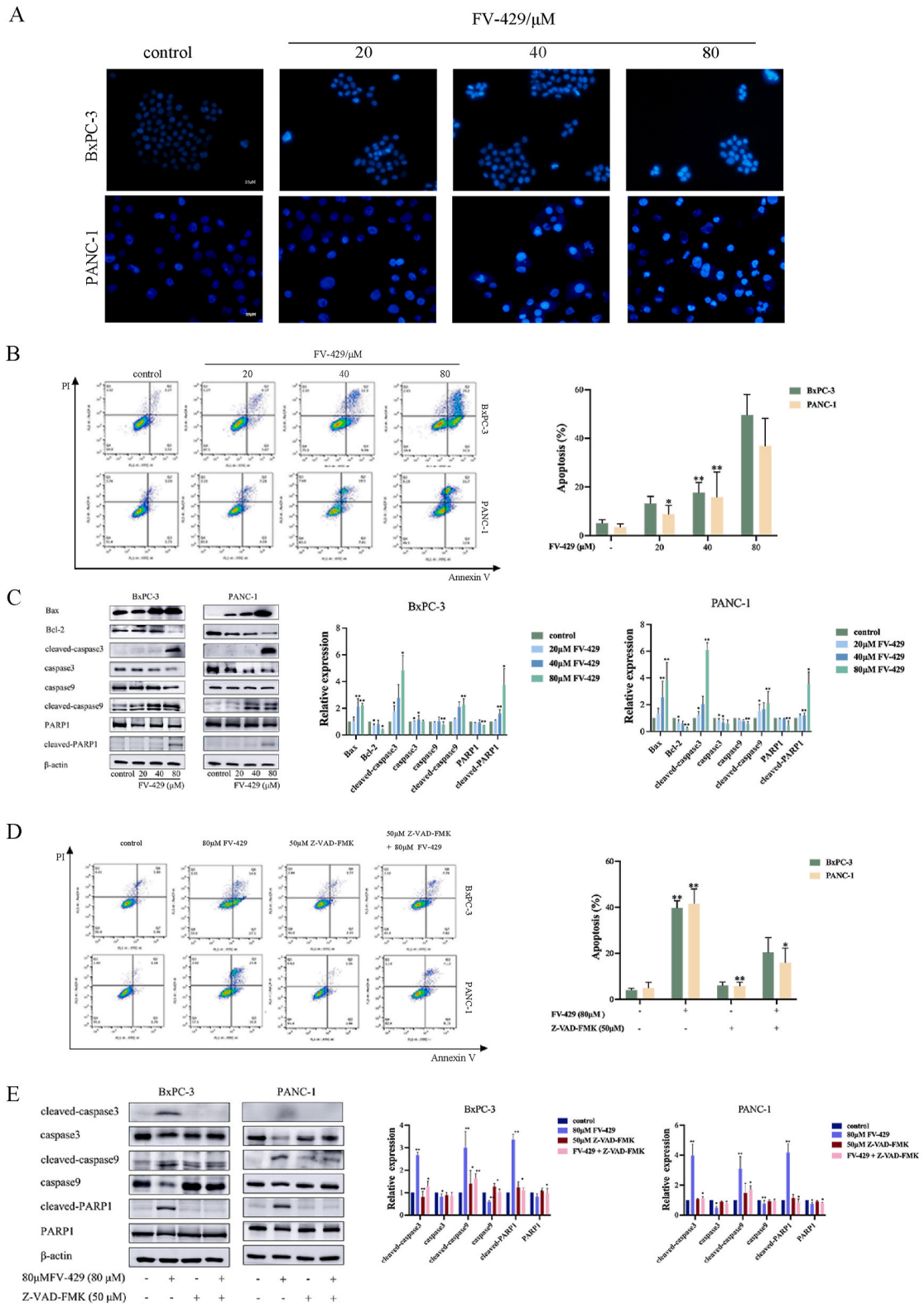
Fig. 2. FV-429 induced mitochondrial apoptosis of PDAC cells. BxPC-3 and PANC-1 cells were exposed to FV-429 (20, 40, and 80 μM) for 24 h. (A) DAPI staining was performed to examine the apoptosis. (B) Apoptosis was measured by Annexin V-FITC/PI and quantified into histogram. (C) Western blotting analysis of caspase3, cleaved-caspase3, caspase9, cleaved-caspase9, cleaved-PARP1, PARP1 , Bax , Bcl-2 and quantified into histogram. Pancreatic cancer BxPC-3 and PANC-1 cells were treated with FV-429 (80 μM) or/and Z-VAD-FMK (50 μM), and the cells were collected

after 24 h. β-actin was used as loading control. (D) Apoptosis was measured by Annexin V-FITC/PI and quantified into histogram. (E) Western blotting analysis of caspase3, cleaved-caspase3, caspase9, cleaved-caspase9, PARP1, cleaved-PARP1 and quantified into histogram. Data are presented as mean ± SD of three independent experiments performed in triplicates. Significant difference: *p < 0.05, **p < 0.01, compared with the control.

Specifically, BxPC-3, PANC-1, and HPNE cells were incubated with different FV-429 concentrations (0–200 μM) for 24 h. The results indicated a significant reduction in cell viability (Fig. 1B). The MTT assay calculated the IC50 values for BxPC-3 and PANC-1 cells at 44.69 ± 1.53 μM and 43.21 ± 1.11 μM, respectively. The IC50 value for HPNE cells was 77.45 ± 1.83 μM (**p < 0.01). We used CCK8 assay to detect the PDAC cell growth. We found that the inhibition was gradually obvious with the increase of concentration (Fig. 1C). Furthermore, the cell number change observed in Fig. 1D indicated that FV-429 treatment (at 20, 40, and 80 μM) for 24 h inhibited the proliferation of BxPC-3 and PANC-1 cells compared with the untreated cells. Upregulation of glycolysis is required for maintaining unlimited cell growth in multiple human cancers. Aerobic glycolysis-mediated glucose catabolism for ATP generation was required for
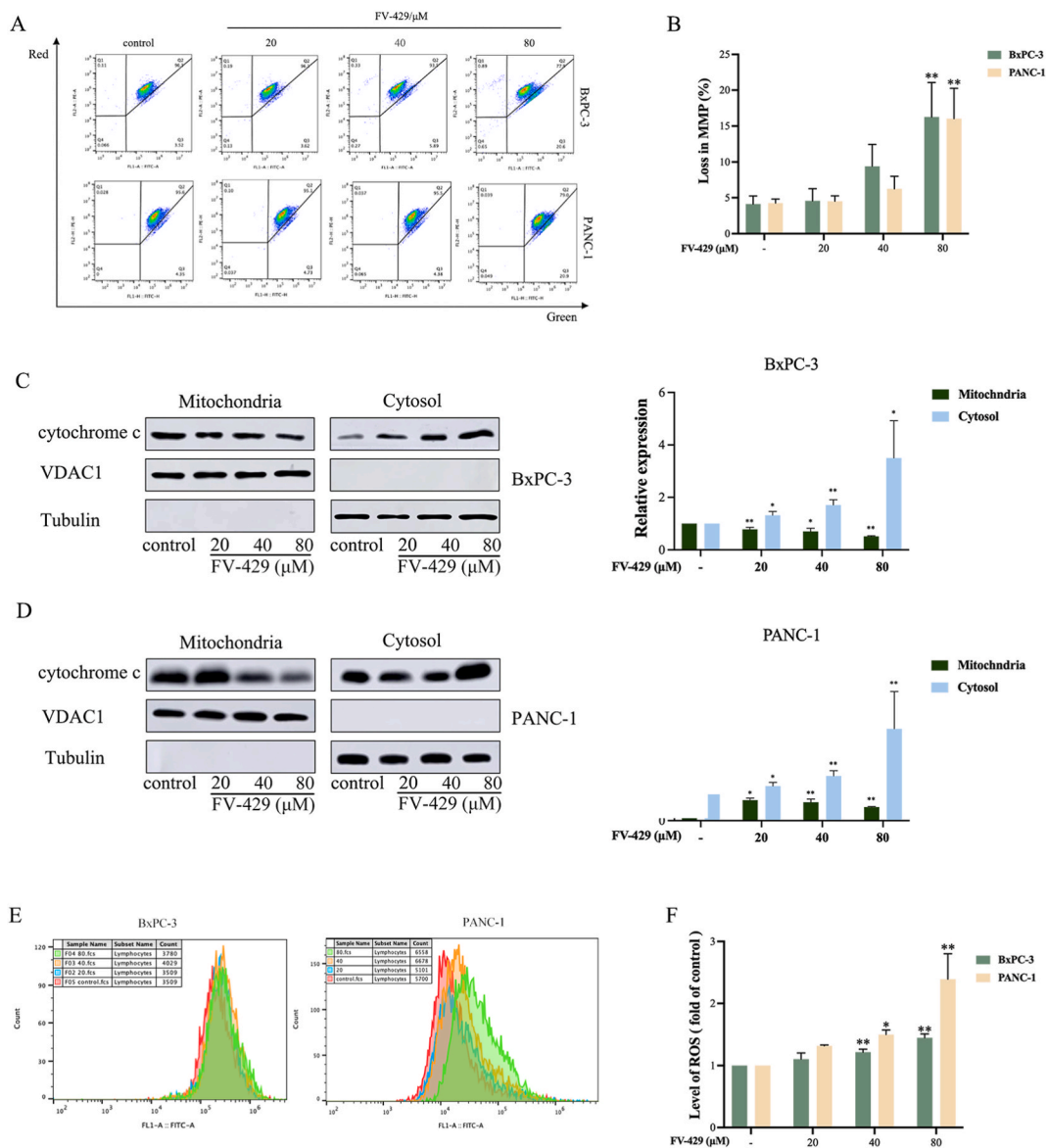

Fig. 3. FV-429 mediated the release of Cyt *c* via mitochondrial membrane potential and ROS. BxPC-3 and PANC-1 cells were exposed to FV-429 (20, 40, and 80 μM for 24 h. (A) JC-1 staining was determined by flow Cytometer. (B) Quantitative analysis of the level of JC-1. (C,D) Mitochondrial protein and cytoplasmic protein were extracted. Western blotting analysis of Cyt *c* and quantified into histogram. (E) ROS level was analyzed by flow Cytometer with DCFH-DA probe. (F) Quantitative analysis of the level of ROS. Data are presented as mean ± SD of three independent experiments performed in triplicates. Significant difference: *p < 0.05, **p < 0.01, compared with the control.

cell proliferation. We therefore investigated the effects of FV-429 on glycolysis and energy metabolism of PDAC cells. These cells were treated with FV-429 for 24 h, which led to morphological changes (Fig. 1D) and inhibition of cell proliferation. This suggested that FV-429 affects glycolysis and energy metabolism in PDAC cells, potentially suppressing their growth.

To investigate the characteristics of FV-429-regulated energy metabolism in PDAC cells, we assessed the levels of substrate consumption and metabolite production. The effects of FV-429 on glucose metabolism and viability were investigated in the PDAC cells. The results confirmed that FV-429 treatment decreased levels of lactate, which is byproduct of glucose metabolism through glycolysis. Additionally, cellular ATP levels were reduced in a dose dependent manner (Fig. 1E and F). Furthermore, glucose consumption was assessed using a Glucose Assay Kit. FV-429 treatment decreased glucose consumption by the PDAC cells (Fig. 1G). This result suggested that FV-429 can reduce the utilization of glucose, a crucial nutrient for cancer cells. To further investigate the impact of FV-429 on glucose metabolism, the extracellular acidification rate (ECAR), an indicator of glycolytic efficiency, was measured. FV-429 suppressed the glycolytic capability of the PDAC cells (Fig. 1G–I). These outcomes demonstrated that FV-429 had the ability to inhibit the glycolysis and viability of PDAC cells.

3.2. FV-429 induced mitochondrial apoptosis of PDAC cells

Glycolysis is important for its promotions of tumorigenesis, and glycolysis maintains survival and progression. When glycolysis is impaired, it cannot provide sufficient biosynthetic precursors for cancer survival, and apoptosis is consequently induced. Because FV-429 inhibited glycolysis and effected morphological changes, we determined whether FV-429 could induce apoptotic cell death in the PDAC cells. Accordingly, we used DAPI staining to visualize apoptosis-associated nuclear changes. Untreated BxPC-3 and PANC-1 cells exhibited round nuclei evenly stained with DAPI (Fig. 2A). However, in the FV-429-treated cells occurring apoptosis, the nuclei appeared fragmented and exhibited more intense staining because of DNA condensation. In addition to DAPI staining, we used Annexin V-FITC/PI staining to further confirm that FV-429 induced apoptosis. We treated the cells with varying FV-429 concentrations (20, 40, and 80 μM) for 24 h and observed an increase in the apoptotic rates of both BxPC-3 and PANC-1 cells with increasing FV-429 concentrations (Fig. 2B) (*p < 0.05, **p < 0.01). These results suggested that FV-429 can induce apoptotic cell death in cancer cells by inhibiting glycolysis. The findings offer valuable insights into the role played by glycolysis in cancer survival and progression. They also highlight FV-429 as a therapeutic agent for targeting this metabolic pathway during cancer treatment.

Meanwhile, after treatment with FV-429 for 24 h, the levels of the anti-apoptotic protein Bcl-2 decreased, whereas those of the pro-apoptotic protein Bax increased in a dose-dependent manner. This shift in protein expression was crucial for triggering mitochondria-mediated apoptosis (Fig. 2C). Specific enzymes involved in apoptosis, namely caspase3, caspase9, and PARP1, were examined for further validation (Fig. 2C). The results exhibited their activation, indicating that FV-429 treatment indeed triggered apoptotic pathways. To confirm whether the observed apoptosis depended on the caspase cascade, Z-VAD-FMK, a pan-caspase inhibitor, was used. Z-VAD-FMK partially reversed FV-429-induced apoptosis, as evidenced through Annexin V-FITC/PI double staining and western blotting (Fig. 2D and E). In conclusion, the study demonstrated that FV-429 induced caspase-dependent PDAC cell apoptosis, primarily through mitochondria-mediated pathways.

3.3. FV-429 mediated the release of cyt c via mitochondrial membrane potential and ROS

To further deliberate the regulation underlying apoptosis in BxPC-3 and PANC-1 cells, the effect of FV-429 on the mitochondrial function was investigated. During the early apoptosis time, the change in the mitochondrial membrane potential (MMP) is indicative of mitochondrial dysfunction. The fluoroscopic probe JC-1 was used for detecting the change in the MMP following FV-429 treatment for 24 h. The results (Fig. 3A and B) revealed that compared with the control group, cell clusters were observed after FV-429 administration, thereby indicating a potential induction of apoptosis. Furthermore, both BxPC-3 and PANC-1 cells exhibited a dose-dependent increase in MMP following FV-429 treatment. These findings suggested that PDAC cells are particularly susceptible to FV-429-induced mitochondrial membrane depolarization. The increased MMP noted in both cell lines implies that FV-429 triggers mitochondrial dysfunction.

Along with changes in the MMP, Cyt *c* would also be released from the outer mitochondrial membrane into the cytoplasm to play a pro-apoptotic role [18,19]. To investigate the specific mechanism underlying FV-429-induced mitochondrial apoptosis, BxPC-3 and PANC-1 cells were treated with FV-429 (20, 40, 80 μM) for 24 h. FV-429 could release Cyt *c* from mitochondria into the cytoplasm of BxPC-3 (Fig. 3C) and PANC-1 (Fig. 3D) cells.

FV-429 treatment possibly leads to dose-dependent ROS accumulation. This oxidative stress caused mitochondrial membrane depolarization, further increasing ROS production and affecting cell viability. The involvement of ROS in apoptosis following FV-429 treatment was therefore important to consider. The previous study we mentioned reported that FV-429 treatment significantly increased cellular ROS levels (Fig. 3E and F). Additionally, FV-429 induced changes in MMP and Cyt *c* release, ultimately leading to mitochondrial dysfunction and apoptosis in BxPC-3 and PANC-1 cells. These findings highlighted the potential mechanisms through which FV-429 induced its effects on cell viability and apoptosis.

3.4. FV-429 reduced the expression of PKM2 and promoted PKM2 nuclear translocation

PK has a significant role in glycolysis, and studies have recently shed light on the specific functions of PK isoform M2 (PKM2) in cellular processes. Briefly, PKM2 was involved in regulating the final glycolysis step to ensure sufficient energy production [20]. Additionally, Li et al. noted that PKM2 promoted mitochondrial fusion and coordinated oxidative phosphorylation while attenuating
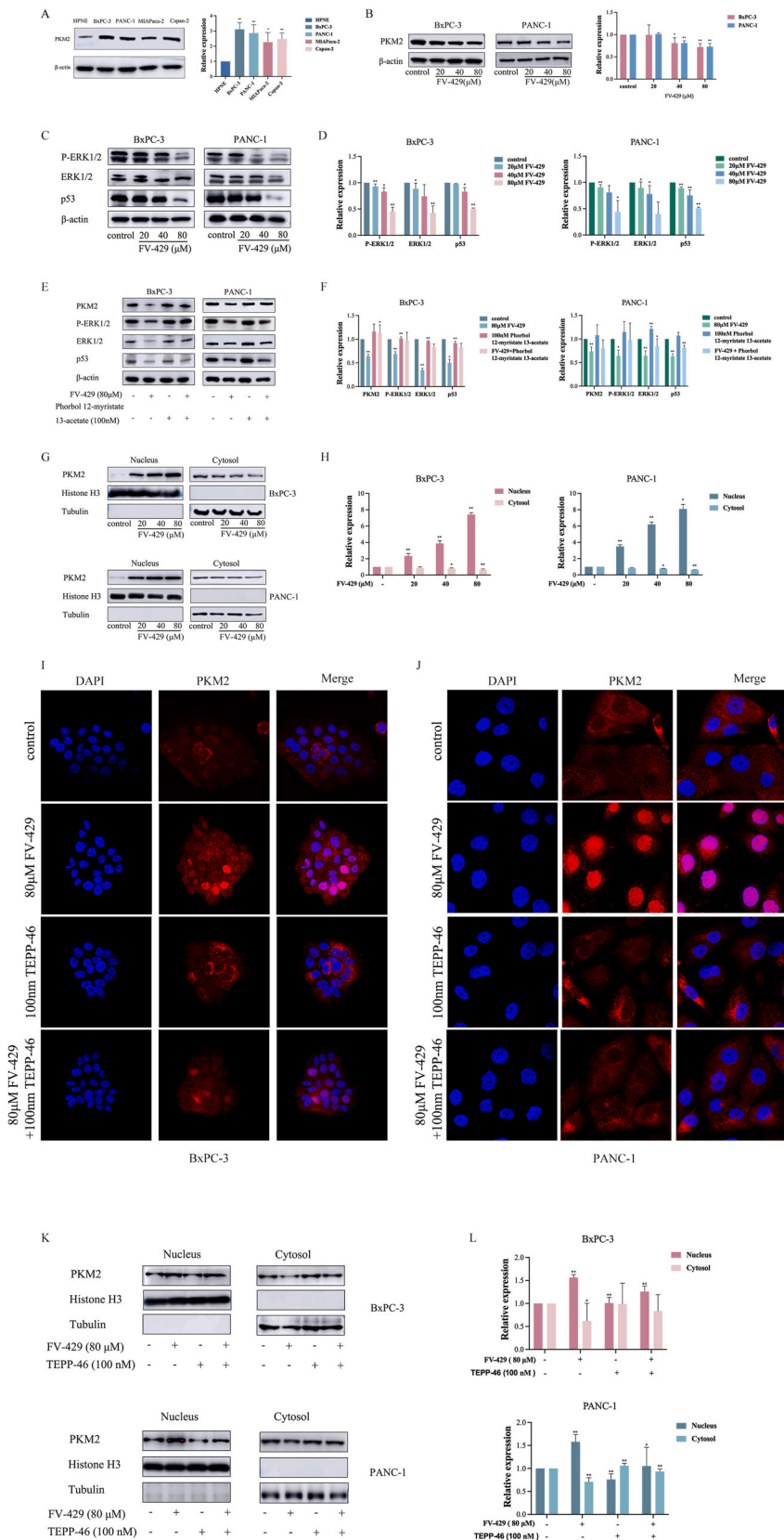
(caption on next page)

Fig. 4. The regulation of FV-429 on PKM2's expression and nuclear translocation. (A) Human normal pancreatic HPNE cells and human pancreatic cancer BxPC-3, PANC-1, MIAPaca-2 and Capan-2 cells were collected after 24 h. Western blotting analysis of PKM2 and quantified into histogram. (B) Pancreatic cancer BxPC-3 and PANC-1 cells were treated with FV-429 at 20, 40, and 80 μM, respectively, and the cells were collected after 24 h. β-actin was used as loading control. Western blotting analysis of PKM2 and quantified into histogram. (C,D) BxPC-3 and PANC-1 cells were exposed to FV-429 (20, 40, and 80 μM for 24 h. Western blotting analysis of P-ERK1/2, ERK1/2, p53, and quantified into histogram. (E,F) Pancreatic cancer BxPC-3 and PANC-1 cells were treated with FV-429 at 80 μM or/and Phorbol 12-myristate 13-acetate at 100 nm, and the cells were collected after 24 h. β-actin was used as loading control. Western blotting analysis of PKM2、P-ERK1/2、ERK1/2 and p53. Quantified into histogram. (G,H) BxPC-3 and PANC-1 cells were exposed to FV-429 (20, 40 and 80 μM) for 24 h. Nuclear protein and cytosol protein were extracted. Western blotting analysis of PKM2 and quantified into histogram. (I,J) Pancreatic cancer BxPC-3 and PANC-1 cells were treated with FV-429 at 80 μM or/and TEPP-46 at 100 nM for 24 h. The content of PKM2 was detected by immunofluorescence assay. Scale bar, 25 μm. (K,L) BxPC-3 and PANC-1 cells were exposed to FV-429 or/and TEPP-46 for 24 h. Nucleoplasmic protein and cytoplasmic protein were extracted. Western blotting analysis of PKM2 and quantified into histogram. Data are presented as mean ± SD of three independent experiments performed in triplicates. Significant difference: $*p < 0.05$, $**p < 0.01$, compared with the control.

glycolysis [21]. Moreover, reducing PKM2 expression could promote nuclear translocation and led to cell cycle arrest and apoptosis [10]. Regarding pancreatic cancer, elevated PKM2 levels were present in the PDAC cells. The PKM2 expression levels were evaluated in human normal pancreatic HPNE cells and PDAC cells, including BxPC-3, PANC-1, MIAPaca-2, and Capan-2 cells. The results revealed abnormal PKM2 upregulation in the PDAC cells (Fig. 4A). To further investigate the effect of PKM2 inhibition, the cells of BxPC-3 and PANC-1 were treated with FV-429 for 24 h, and the change in PKM2 levels was assessed. Fig. 4B indicates a dose-dependent reduction in PKM2 expression following FV-429 treatment.

These findings suggested that targeting PKM2, such as by using FV-429, is a potential therapeutic strategy against pancreatic cancer.

The aforementioned experiments confirmed that FV-429 can downregulate PKM2 expression. Some studies have shown that downregulating the ERK/PKM2/Bcl-2 axis led to the antimelanoma effect [14]. Additionally, MyD88-dependent CCL20, secreted by myofibroblasts, has been suggested to enhance aerobic glycolysis through the ERK/PKM2 signaling pathway [22]. Moreover, studies have reported that PKM2 is dependent on ERK for regulating glycolysis, and its expression is linked to p53 expression and mitochondrial fusion [23]. Other experiments have demonstrated that PKM2 is related to p53 expression and affects mitochondrial fusion [24]. To investigate the potential of FV-429 in modulating the ERK signaling pathway, western blot experiments were conducted after 24 h treatment with FV-429. A downregulation of P-ERK1/2, ERK1/2, and p53 protein levels was observed following FV-429 treatment (Fig. 4C and D). These findings suggest that FV-429 can inhibit the ERK signaling pathway in PDAC cells and can affect the tumor suppressor gene p53.

To further investigate the effect of FV-429 on the association between the ERK signaling pathway and PKM2, phorbol 12-myristate 13-acetate (100 nm), an activator of the ERK signaling pathway, was added to verify the association. PKM2 expression decreased after FV-429 treatment, whereas it increased after treatment with phorbol 12-myristate 13-acetate (Fig. 4E and F). Phorbol 12-myristate 13-acetate reversed the decrease in PKM2 and p53 levels, which was induced by FV-429. These results suggest that FV-429 can reduce PKM2 expression in BxPC-3 and PANC-1 cells through the ERK signaling pathway and can be reversed by the activator of this pathway.

Reducing PKM2 expression and promoting nuclear translocation can cause cell cycle arrest and apoptosis [10]. To investigate whether FV-429 regulates the entry of PKM2 into the nucleus, BxPC-3 and PANC-1 cells were treated with FV-429 and PKM2 levels in the nucleus were tested. After treatment with FV-429, PKM2 was transferred from the cytoplasm into the nucleus (Fig. 4G and H), which suggested that FV-429 induced the nuclear localization of PKM2. To further understand the regulatory mechanism, the cells were treated with TEPP-46, a PKM2 activator. Then, we conducted immunofluorescence and western blot experiments. The addition of TEPP-46 reversed PKM2 nucleation induced by (Fig. 4I and J). This was also verified through western blot analysis (Fig. 4K and L).

The study suggested that FV-429 reduces PKM2 expression through the ERK signaling pathway. This pathway is involved in various cellular processes, including cell growth and survival. In summary, FV-429 appears to regulate PKM2 by inducing its nuclear localization and potentially reducing its expression through the ERK signaling pathway.

3.5. PKM2 played an important role in regulating glycolysis and FV-429-induced mitochondrial apoptosis

Based on the experimental results, PKM2 played a key role in the rate-limiting step of glycolysis and could produce more ATP and lactic acid, which could stimulate tumor cell growth. In view of the aforementioned existing experimental results and the role of PKM2 in pancreatic cancer development in humans, the effects of the PKM2 activator on ATP and lactic acid were examined. BxPC-3 and PANC-1 cells were treated with 80 μM FV-429 or/and 100 nM TEPP-46 for 24 h, and the ATP detection kit was used to detect changes in ATP levels. FV-429 reduced ATP production in the PDAC cells, and ATP production was inhibited by TEPP-46 (Fig. 5A). Similarly, the lactic acid detection kit was used for detecting changes in lactic acid content following treatment with FV-429 and TEPP-46. The results unveiled that FV-429 reduced lactic acid production in the PDAC cells, and lactic acid production was inhibited after TEPP-46 was added (Fig. 5B). Taken together, these findings indicated that FV-429 can modulate glycolytic products, particularly ATP and lactic acid. These results support the growing evidence that PKM2 and glycolysis are involved in pancreatic cancer development, highlighting the potential of PKM2 modulation as a therapeutic strategy against tumor metabolism.

Based on the results, we investigated the relationship between PKM2 and cell caspase family proteins in the context of glycolysis and apoptosis (Fig. 5C and D). The findings revealed that the PKM2 expression decreased after 24 h of FV-429 treatment while it increased after treatment with TEPP-46. Furthermore, the expression of caspase3, caspase9, and PARP1 decreased after FV-429
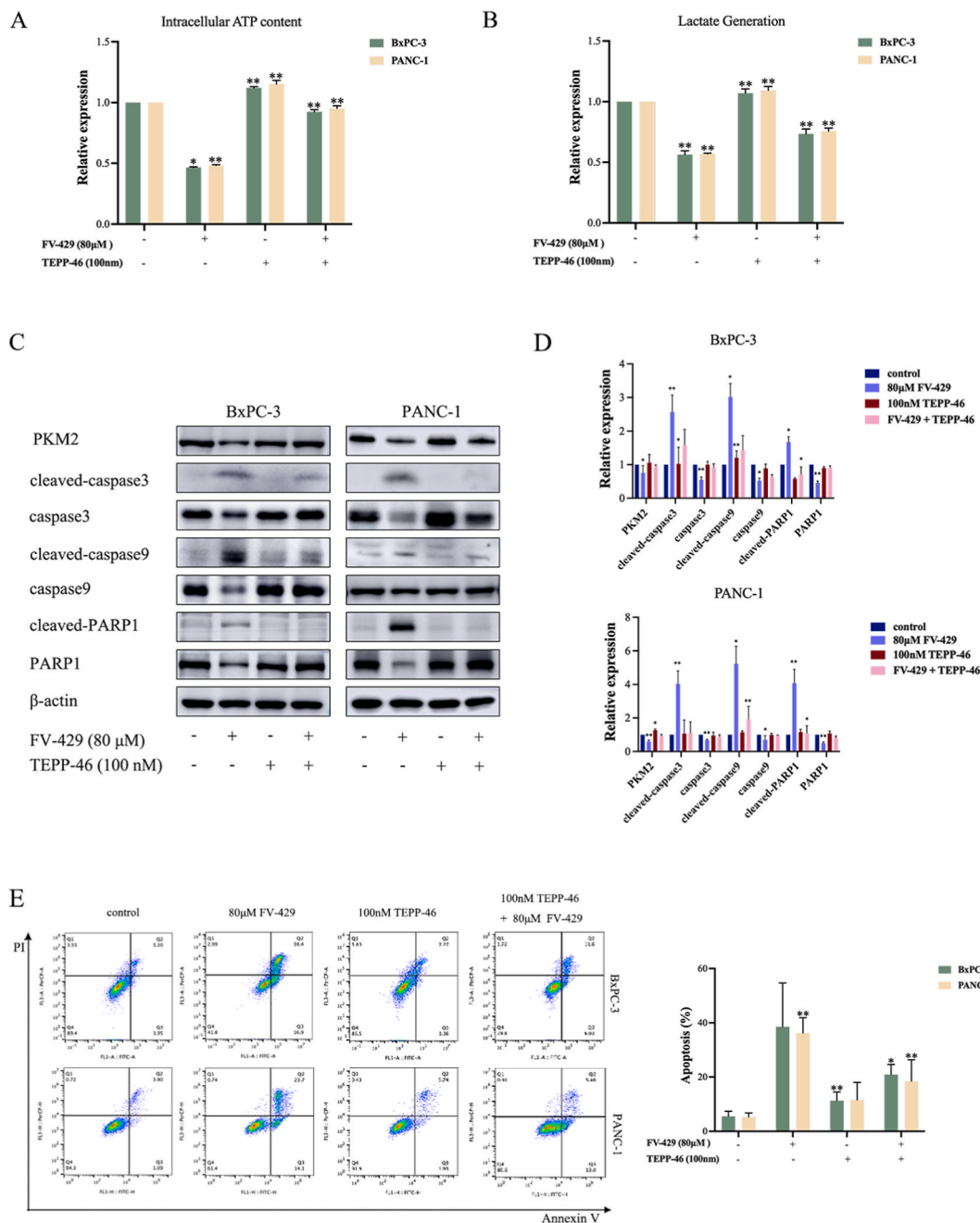
Fig. 5. PKM2 played a key role in the regulation of glycolysis and mitochondrial apoptosis by FV-429. BxPC-3 and PANC-1 cells were treated with FV-429 at 80 μM or/and TEPP-46 at 100 nM, and the cells were collected after 24 h. (A) ATP production was assayed by ATP assay kit. (B) Production of lactic acid was assayed by Lactic Acid production Detection kit. (C,D) Western blotting analysis of PKM2, cleaved-caspase3, caspase3, cleaved-caspase9, caspase9, cleaved-PARP1, PARP1 and quantified into histogram. (E) Annexin V-FITC/PI double staining was determined by flow Cytometer and quantified into histogram. Data are presented as mean ± SD of three independent experiments performed in triplicates. Significant difference: *$p < 0.05$, **$p < 0.01$, compared with the control.

treatment, whereas that of cleaved-caspase3, cleaved-caspase9, and cleaved-PARP1 increased. Importantly, the reversal of FV-429-induced expression of the caspase family protein was achieved with TEPP-46. This suggested that PKM2 played a crucial role in regulating FV-429-mediated mitochondrial apoptosis.

To determine the impact of FV-429 on the PDAC cells and investigate the role of PKM2 nuclear translocation in FV-429-induced apoptosis, BxPC-3 and PANC-1 cells were treated with FV-429 and/or TEPP-46 for 24 h, followed by an Annexin V-FITC/PI assay.
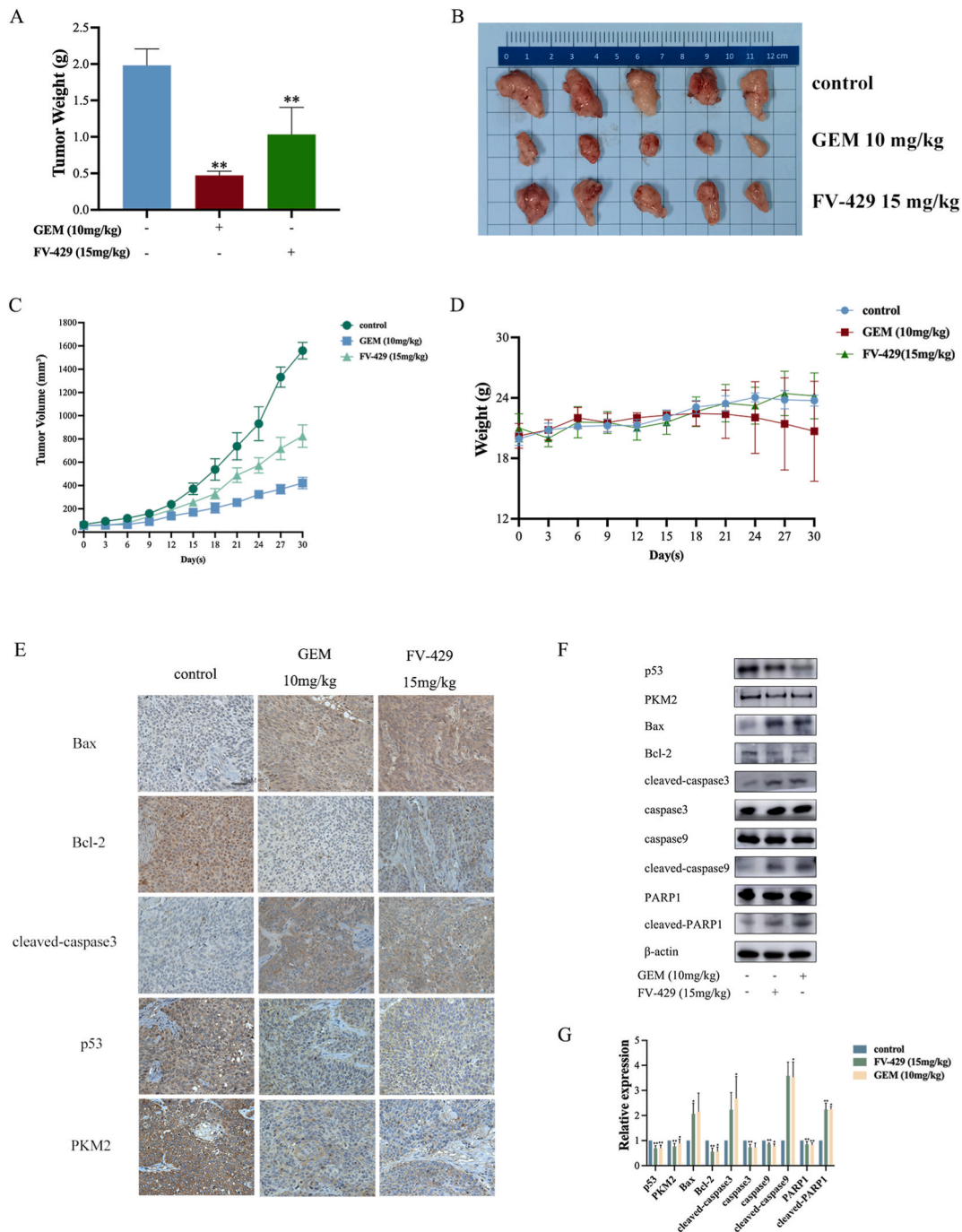
Fig. 6. FV-429 inhibited pancreatic tumor growth *in vivo* and exerted lower toxicity. The xenograft model of human BxPC-3 cells in nude mice was established and administered for 30 days after inoculation. The tumor volume was measured every three days and body weight was recorded. After administration, the mice were killed, and the transplanted tumors in the armpits were dissected and weighed. (A) The weight of tumor for three groups of animals were compared. (B) Tumor exfoliated from nude mice after 30 days treatment. Each group contained 5 mice. (C) The tumor volume were measured once every three days. (D) The body weight of mice was measured once every three days within 30 days of administration. (E) The expression of mitochondrial apoptosis related proteins in tumor xenograft tissues was measured by immunohistochemistry. Scale bars, 50 μm. (F) The tissue protein was extracted and tested. β-actin was used as loading control. Western blots analysis of P53, PKM2, Bax, cleaved-caspase3, caspase3, caspase9, cleaved-caspase9, PARP1 and cleaved-PARP1 in tumor xenograft tissues. (G) Quantified into histogram. Data are presented as mean ± SD of three independent experiments performed in triplicates. Significant difference: *p < 0.05, **p < 0.01, compared with the control.

A significant increase in apoptosis was noted after FV-429 treatment (Fig. 5E), indicating that FV-429 effectively induces apoptosis in the PDAC cells. Notably, the addition of TEPP-46 reversed FV-429-induced apoptosis. Building on previous findings that FV-429 induces PKM2 nuclear translocation, which was reversed by TEPP-46, we concluded that FV-429 promoted PKM2 nuclear translocation and triggered mitochondrial apoptosis in PDAC cells.

In summary, FV-429 exhibited dual effects on PDAC cells. It reduced PKM2 expression, leading to glycolysis inhibition, and induced PKM2 nuclear translocation, triggering mitochondrial apoptosis. Thus, PKM2 played a vital role in regulating both glycolysis and mitochondrial apoptosis in PDAC cells in response to FV-429 treatment.

3.6. FV-429 inhibited pancreatic tumor growth in vivo and exerted lower toxicity

To assess the efficacy and safety of FV-429 *in vivo*, xenograft models were established in nude mice. The effects of the treatment with FV-429 on BxPC-3-transplanted tumors were observed over 30 days. Following FV-429 treatment for 30 days, we killed the mice. Their tumors were excised for experimental analysis. Both FV-429 and gemcitabine, a positive control drug, significantly reduced the tumor volume and weight (Fig. 6A, B, and C). This suggested that FV-429 exerts its antitumor properties in a dose-dependent manner. Moreover, the study assessed FV-429 safety by monitoring the body weight of the nude mice during treatment. Interestingly, only in the group treated with the positive control drug, body weight decreased with increasing administration times (Fig. 6D). By contrast, the FV-429-treated group exhibited no significant difference in body weight compared with the control group, indicating that FV-429 exhibited good safety at therapeutic doses. Overall, these findings suggested that FV-429 effectively inhibits BxPC-3 cell growth *in vivo* and has a favorable safety profile, highlighting its potential as a promising antitumor agent.

Our study results suggest that FV-429 significantly affects the growth of human pancreatic cancer *in vivo*. To investigate this effect further, immunohistochemical and western blot experiments on extracted tumor protein. The immunohistochemical experiments revealed that the levels of Bax and cleaved-caspase3 (Fig. 6E), which were markers of apoptosis, increased after FV-429 treatment. On the other hand, Bcl-2, p53, and PKM2 levels decreased. These findings indicated that FV-429 promotes mitochondrial apoptosis and affects key proteins involved in this process. Furthermore, the western blot analysis confirmed these results and demonstrated that FV-429 significantly influenced the protein levels of various mitochondrial apoptosis-related proteins compared with the control group (Fig. 6F and G). FV-429 upregulated the protein levels of cleaved-caspase3, cleaved-caspase9, Bax, and cleaved-PARP1, which were all associated with apoptosis induction. By contrast, FV-429 significantly downregulated the p53, PKM2, Bcl-2, caspase3, caspase9, and PARP1 protein levels.

Overall, our findings suggested that FV-429 exhibited antitumor effects with lower toxicity and more security in the BxPC-3-inoculated xenograft mice. These consequences supported the potential of FV-429 as a therapeutic option for pancreatic cancers.

4. Discussion

Wogonin, a natural mixture derived from the medicinal plant *S. baicalensis* Georgi. It has shown promising potential as an anti-cancer agent. It can induce apoptosis [25,26], a programmed cell death, in various cancer cell lines while sparing normal human cells [27,28]. Wogonin exhibits low water solubility and exhibits optimal efficacy at relatively high doses, which has hindered its widespread usage. Interestingly, the role of Wogonin in glycolysis and apoptosis specifically in pancreatic cancer has not been extensively explored. Glycolysis is a metabolic pathway, and cancer cells often rely on it for energy production and sustained growth. Investigating how Wogonin influences glycolytic activity and apoptosis in PDAC cells could provide valuable insights into its therapeutic potential for pancreatic cancer. These trials evaluated its safety, efficacy, and dosage requirements in a larger patient population. If the trial results are satisfactory, Wogonin could become a novel treatment option for cancer patients, potentially overcoming its limitations such as high required doses.

Therefore, we found a derivative of Wogonin, FV-429, has promising stability and efficacy. We here reported the special glycolytic inhibition and apoptosis-inducing effects of FV-429 on PDAC cells. This was achieved by regulating the key rate-limiting enzyme PKM2 in glycolysis. FV-429 downregulated PKM2 expression by inhibiting the ERK signaling pathway and induced PKM2 nuclear translocation. The inhibition of glycolytic metabolite production and the induction of mitochondrial apoptosis are key mechanisms by which FV-429 exerted its anticancer effects on PDAC cells. FV-429 inhibited the production of glycolytic metabolites by decreasing PKM2 expression, and led to the entry of PKM2 into the nucleus, which induced PDAC cell apoptosis. Along with pancreatic cancer, FV-429 has also been studied in other cancer types. In hepatocellular carcinoma cells (HepG2), FV-429 has shown inhibitory effects [29]. FV-429 can also reverse drug resistance in PDAC cells by inhibiting c-Src [30]. Additionally, FV-429 regulates glycolysis inhibition and induces apoptosis in human prostate cancer cells through the AR-AKT-HK2 signaling network [31]. In another study, FV-429 induced apoptosis in PDAC cells via the AKT-SREBP1-FASN signaling network [32]. These studies have highlighted the potential role of FV-429 in metabolic regulation to enhance highly effective and low-toxicity antitumor drugs that better align with clinical requirements. Continued research on FV-429 and its action mechanisms could contribute to the development of novel therapeutic strategies against cancer.

Pancreatic cancer has a complex pathogenesis that remains incompletely understood. Despite various treatment interventions, such as radiotherapy, chemotherapy, and surgery, are used for treatment, the cure rate for pancreatic cancer remains low, thereby highlighting the need for alternative therapies and biomarkers for improving patient outcomes. We hypothesized that targeting both glycolysis (a metabolic pathway) and apoptosis (programmed cell death) with less toxic drugs could potentially inhibit the progression of cancer. We here investigated the effects of FV-429 on PDAC cells. FV-429 led to morphological changes in the PDAC cells, indicating its impact on the cell structure. The drug's effectiveness was confirmed in the MTT analysis, which revealed that FV-429 inhibited

PDAC cell proliferation. In fact, we noted that FV-429 could inhibit glycolysis. Additionally, FV-429 treatment induced apoptosis, as evidenced through various assays such as DAPI, Annexin V-FITC/PI, and western blotting. Further investigation into the cellular mechanisms found that FV-429 induced apoptosis by generating ROS and subsequent mitochondrial apoptosis. This finding sparked an interest in exploring the interplay between glycolysis and mitochondrial apoptosis, thereby suggesting a potential link between these two biological processes in PDAC cells.

PK is a rate-limiting enzyme in the final glycolysis step. Which can transfer phosphate groups from phosphoenolpyruvate to adenosine diphosphate to produce pyruvate. PKM2 is generally highly expressed in tumor cells as a low activity dimer [9]. As a key metabolic kinase in the "Warburg effect" of tumor cells, PKM2 controls the last step of glycolysis to ensure adequate energy supply [20]. The flavonoid breviscapine [10] promoted PKM2 nuclear translocation and induced G2/M phase cell cycle arrest and apoptosis of HeLa cells. Considering that glycolysis is affected by the rate-limiting enzyme PKM2 and that a complex interaction and regulation exists between glycolysis and apoptosis, we first analyzed PKM2 expression in different clinical tumor samples and then in different human pancreatic cancer cells through the HPA database. PKM2 expression in tumor tissues was abnormally increased. Furthermore, the ERK signaling pathway regulates PKM2 localization and influences cell proliferation, differentiation, migration, senescence, and apoptosis [33]. ERK could also affect tumor the suppressor gene p53 and cell proliferation and apoptosis [34]. It could induce G2/M phase cell cycle arrest and apoptosis of HeLa cells [20]. Moreover, the PKM2 activator TEPP-46 was added to analyze the entry of PKM2 into the nucleus. The addition of TEPP-46 reversed the entry of FV-429-induced PKM2, indicating that FV-429 regulates PKM2 nuclear translocation.

We then hypothesized a connection between cellular glycolysis and apoptosis by PKM2. In view of the aforementioned existing experimental results, we examined changes in glycolytic metabolites following the addition of FV-429 or/and TEPP-46. The addition of FV-429 resulted in the inhibition of lactic acid and ATP production, whereas TEPP-46 reversed this effect, highlighting the role of PKM2 in this process. To further investigate the relationship between glycolysis and apoptosis, the connection between PKM2 and caspase family proteins was explored. Addition of the PKM2 activator, TEPP-46, reversed the FV-429-induced changes in caspase family protein expression. Additionally, the Annexin V-FITC/PI confirmed that TEPP-46 counteracted the FV-429-induced apoptosis of pancreatic cancer cells. To summarize, we here confirmed that FV-429 inhibited glycolysis by reducing PKM2 expression, with the ERK signaling pathway playing a significant role. Furthermore, FV-429 promoted nuclear translocation of PKM2, thereby inducing apoptosis in human pancreatic cancer cells. This information provides valuable insights into the potential therapeutic strategy of targeting glycolysis and PKM2 in pancreatic cancer treatment.

In addition, we investigated the *in vivo* action of FV-429. The antitumor effects of FV-429 and gemcitabine were evaluated in BxPC-3-inoculated xenograft mice. According to the results, FV-429 could inhibit the growth of solid tumors *in vivo* and is associated with a strong safety.

In summary, our research revealed that FV-429 has a good glycolytic inhibitory activity and mitochondrial apoptosis-inducing effect in pancreatic cancers *in vivo* and *in vitro*.

5. Conclusion

In conclusion, FV-429 played an important role in strong antitumor effects. FV-429 reduced PKM2 expression by inhibiting the ERK signaling network and promoted its nuclear translocation. Furthermore, FV-429 exerted antitumor effects with lower toxicity and more safety in the BxPC-3-inoculated xenograft mice. Our outcomes provided a different insight that FV-429 stops pancreatic cancer development by efficaciously disrupting glycolysis and simultaneously inducing cell apoptosis. This strongly Thank you very much for your consideration of this work. Any suggestions will be greatly appreciated. Looking forward to your reply!Thank you very much for your consideration of this work. Any suggestions will be greatly appreciated. Looking forward to your reply! the use of FV-429 as a therapy for pancreatic cancer.

Funding

Availability of data and materials

All data will be shared upon reasonable request to the corresponding author. The datasets used and/or analyzed during the current study are available from the corresponding author on reasonable request.

Ethical statement

All mouse experiments were in compliance with the policies of the SFDA (State Food and Drug Administration) of China on Animal Care. All animals received humane care according to the criteria outlined in the Guide for the Care and Use of Laboratory Animals prepared by the National Academy of Sciences and published by the National Institutes of Health. Female athymic nude mice (4–6 weeks old) weighing 18–22 g were purchased from the Academy of Military Medical Sciences of the Chinese People's Liberation Army (Certificate No. SCXK(ZHE) 2019–0004).

CRediT authorship contribution statement

Xifan Jin: Writing – review & editing, Writing – original draft, Visualization, Validation, Supervision, Software, Resources, Project administration, Methodology, Investigation, Funding acquisition, Formal analysis, Data curation, Conceptualization. **Qi Min:** Software, Resources, Project administration, Methodology, Investigation, Funding acquisition, Formal analysis, Data curation. **Dechao Wang:** Validation, Supervision, Project administration, Methodology, Investigation, Conceptualization. **Yi Wang:** Writing – review & editing, Validation, Resources, Investigation, Conceptualization. **Guangming Li:** Writing – review & editing, Visualization, Validation, Resources, Conceptualization. **Zhiying Wang:** Software, Project administration, Investigation, Data curation. **Yongjian Guo:** Writing – review & editing, Writing – original draft, Visualization, Validation. **Yuxin Zhou:** Writing – review & editing, Writing – original draft, Visualization, Validation, Supervision.

Declaration of competing interest

The authors declare that they have no known competing financial interests or personal relationships that could have appeared to influence the work reported in this paper.

Appendix A. Supplementary data

Supplementary data to this article can be found online at https://doi.org/10.1016/j.heliyon.2024.e29515.

References

[1] W. Chen, et al., Cancer statistics in China, 2015, CA A Cancer J. Clin. 66 (2016) 115–132, https://doi.org/10.3322/caac.21338.
[2] X. Bian, et al., Prognostic values of abdominal body compositions on survival in advanced pancreatic cancer, Medicine 97 (2018) e10988, https://doi.org/10.1097/md.0000000000010988.
[3] C.J. Halbrook, C.A. Lyssiotis, Employing metabolism to improve the diagnosis and treatment of pancreatic cancer, Cancer Cell 31 (2017) 5–19, https://doi.org/10.1016/j.ccell.2016.12.006.
[4] R.A. Lockshin, C.M. Williams, Programmed cell death–I. Cytology of degeneration in the intersegmental muscles of the pernyi SILKMOTH, J. Insect Physiol. 11 (1965) 123–133, https://doi.org/10.1016/0022-1910(65)90099-5.
[5] D.P. Del Re, D. Amgalan, A. Linkermann, Q. Liu, R.N. Kitsis, Fundamental mechanisms of regulated cell death and implications for heart disease, Physiol. Rev. 99 (2019) 1765–1817, https://doi.org/10.1152/physrev.00022.2018.
[6] X. Liu, C.N. Kim, J. Yang, R. Jemmerson, X. Wang, Induction of apoptotic program in cell-free extracts: requirement for dATP and cytochrome c, Cell 86 (1996) 147–157, https://doi.org/10.1016/s0092-8674(00)80085-9.
[7] O. Warburg, F. Wind, E. Negelein, The metabolism of tumors in the body, J. Gen. Physiol. 8 (1927) 519–530, https://doi.org/10.1085/jgp.8.6.519.
[8] E. Panieri, M.M. Santoro, ROS homeostasis and metabolism: a dangerous liaison in cancer cells, Cell Death Dis. 7 (2016) e2253, https://doi.org/10.1038/cddis.2016.105.
[9] T.L. Dayton, T. Jacks, M.G. Vander Heiden, PKM2, cancer metabolism, and the road ahead, EMBO Rep. 17 (2016) 1721–1730, https://doi.org/10.15252/embr.201643300.
[10] L. You, et al., Scutellarin inhibits Hela cell growth and glycolysis by inhibiting the activity of pyruvate kinase M2, Bioorg. Med. Chem. Lett 27 (2017) 5404–5408, https://doi.org/10.1016/j.bmcl.2017.11.011.
[11] D. Anastasiou, et al., Pyruvate kinase M2 activators promote tetramer formation and suppress tumorigenesis, Nat. Chem. Biol. 8 (2012) 839–847, https://doi.org/10.1038/nchembio.1060.
[12] P. Wang, C. Sun, T. Zhu, Y. Xu, Structural insight into mechanisms for dynamic regulation of PKM2, Protein & cell 6 (2015) 275–287, https://doi.org/10.1007/s13238-015-0132-x.
[13] W. Yang, et al., ERK1/2-dependent phosphorylation and nuclear translocation of PKM2 promotes the Warburg effect, Nat. Cell Biol. 14 (2012) 1295–1304, https://doi.org/10.1038/ncb2629.
[14] H. Zhao, et al., Resveratrol induces apoptosis in human melanoma cell through negatively regulating Erk/PKM2/Bcl-2 axis, OncoTargets Ther. 11 (2018) 8995–9006, https://doi.org/10.2147/ott.S186247.
[15] C.D. Lucas, et al., Wogonin induces eosinophil apoptosis and attenuates allergic airway inflammation, Am. J. Respir. Crit. Care Med. 191 (2015) 626–636, https://doi.org/10.1164/rccm.201408-1565OC.
[16] S.C. Fas, et al., Wogonin sensitizes resistant malignant cells to TNFalpha- and TRAIL-induced apoptosis, Blood 108 (2006) 3700–3706, https://doi.org/10.1182/blood-2006-03-011973.
[17] Y. Zhou, et al., FV-429 induces apoptosis and inhibits glycolysis by inhibiting Akt-mediated phosphorylation of hexokinase II in MDA-MB-231 cells, Mol. Carcinog. 55 (2016) 1317–1328, https://doi.org/10.1002/mc.22374.
[18] S. Dadsena, et al., Ceramides bind VDAC2 to trigger mitochondrial apoptosis, Nat. Commun. 10 (2019) 1832, https://doi.org/10.1038/s41467-019-09654-4.
[19] P.P. Praharaj, et al., Intricate role of mitochondrial lipid in mitophagy and mitochondrial apoptosis: its implication in cancer therapeutics, Cell. Mol. Life Sci. : CM 76 (2019) 1641–1652, https://doi.org/10.1007/s00018-018-2990-x.
[20] Z. Zhang, et al., PKM2, function and expression and regulation, Cell Biosci. 9 (2019) 52, https://doi.org/10.1186/s13578-019-0317-8.
[21] T. Li, et al., PKM2 coordinates glycolysis with mitochondrial fusion and oxidative phosphorylation, Protein & cell 10 (2019) 583–594, https://doi.org/10.1007/s13238-019-0618-z.
[22] Q. Yuan, et al., MyD88 in myofibroblasts regulates aerobic glycolysis-driven hepatocarcinogenesis via ERK-dependent PKM2 nuclear relocalization and activation, J. Pathol. 256 (2022) 414–426, https://doi.org/10.1002/path.5856.
[23] T.L. Wong, et al., CRAF methylation by PRMT6 regulates aerobic glycolysis-driven hepatocarcinogenesis via ERK-dependent PKM2 nuclear relocalization and activation, Hepatology 71 (2020) 1279–1296, https://doi.org/10.1002/hep.30923.
[24] H. Wu, et al., Overexpression of PKM2 promotes mitochondrial fusion through attenuated p53 stability, Oncotarget 7 (2016) 78069–78082, https://doi.org/10.18632/oncotarget.12942.
[25] R. Kumar, et al., Fascinating chemopreventive story of wogonin: a chance to hit on the head in cancer treatment, Curr. Pharmaceut. Des. 27 (2021) 467–478, https://doi.org/10.2174/1385272824999200427083040.
[26] X.S. Du, et al., Wogonin attenuates liver fibrosis via regulating hepatic stellate cell activation and apoptosis, Int. Immunopharm. 75 (2019) 105671, https://doi.org/10.1016/j.intimp.2019.05.056.

[27] Q. Zhao, et al., Two CYP82D enzymes function as flavone hydroxylases in the biosynthesis of root-specific 4'-deoxyflavones in Scutellaria baicalensis, Mol. Plant 11 (2018) 135–148, https://doi.org/10.1016/j.molp.2017.08.009.

[28] S. Baumann, et al., Wogonin preferentially kills malignant lymphocytes and suppresses T-cell tumor growth by inducing PLCgamma1- and Ca2+-dependent apoptosis, Blood 111 (2008) 2354–2363, https://doi.org/10.1182/blood-2007-06-096198.

[29] Z. Yang, et al., Reactive oxygen species-mitochondria pathway involved in FV-429-induced apoptosis in human hepatocellular carcinoma HepG2 cells, Anti Cancer Drugs 22 (2011) 886–895, https://doi.org/10.1097/CAD.0b013e3283483d65.

[30] Q. Guo, et al., Influence of c-Src on hypoxic resistance to paclitaxel in human ovarian cancer cells and reversal of FV-429, Cell Death Dis. 8 (2018) e3178, https://doi.org/10.1038/cddis.2017.367.

[31] X. Chen, et al., Glycolysis inhibition and apoptosis induction in human prostate cancer cells by FV-429-mediated regulation of AR-AKT-HK2 signaling network, Food Chem. Toxicol. : an international journal published for the British Industrial Biological Research Association 143 (2020) 111517, https://doi.org/10.1016/j.fct.2020.111517.

[32] Y. Sun, et al., Apoptosis induction in human prostate cancer cells related to the fatty acid metabolism by wogonin-mediated regulation of the AKT-SREBP1-FASN signaling network, Food Chem. Toxicol. : an international journal published for the British Industrial Biological Research Association 169 (2022) 113450, https://doi.org/10.1016/j.fct.2022.113450.

[33] H.C. Pan, et al., Quercetin promotes cell apoptosis and inhibits the expression of MMP-9 and fibronectin via the AKT and ERK signalling pathways in human glioma cells, Neurochem. Int. 80 (2015) 60–71, https://doi.org/10.1016/j.neuint.2014.12.001.

[34] X. Hou, et al., The involvement of ERK1/2 and p38 MAPK in the premature senescence of melanocytes induced by H(2)O(2) through a p53-independent p21 pathway, J. Dermatol. Sci. 105 (2022) 88–97, https://doi.org/10.1016/j.jdermsci.2022.01.002.